

# Plastid proteins crucial for symbiotic fungal and bacterial entry into plant roots

Haruko Imaizumi-Anraku<sup>1,2,\*</sup>, Naoya Takeda<sup>3,\*</sup>, Myriam Charpentier<sup>4,†</sup>, Jillian Perry<sup>4</sup>, Hiroki Miwa<sup>5</sup>, Yosuke Umehara<sup>1,6</sup>, Hiroshi Kouchi<sup>1,6</sup>, Yasuhiro Murakami<sup>1,2</sup>, Lonneke Mulder<sup>4</sup>, Kate Vickers<sup>4</sup>, Jodie Pike<sup>4</sup>, J. Allan Downie<sup>5</sup>, Trevor Wang<sup>5</sup>, Shusei Sato<sup>7</sup>, Erika Asamizu<sup>7</sup>, Satoshi Tabata<sup>7</sup>, Makoto Yoshikawa<sup>3</sup>, Yoshikatsu Murooka<sup>3</sup>, Guo-Jiang Wu<sup>3</sup>, Masayoshi Kawaguchi<sup>6,8</sup>, Shinji Kawasaki<sup>1,2</sup>, Martin Parniske<sup>4,†</sup> & Makoto Hayashi<sup>3,6</sup>

<sup>1</sup>National Institute of Agrobiological Sciences, 2-1-2 Kannondai, Tsukuba, Ibaraki 305-8602, Japan  
<sup>2</sup>Bio-oriented Technology Research Advancement Institution (BRAIN), Tokyo Office, 3-18-19 Toranomon Minato-ku, Tokyo 105-0001, Japan  
<sup>3</sup>Department of Biotechnology, Graduate School of Engineering, Osaka University, 2-1 Yamadaoka, Suita, Osaka 565-0871, Japan  
<sup>4</sup>The Sainsbury Laboratory, John Innes Centre, Colney Lane, Norwich NR4 7UH, UK  
<sup>5</sup>John Innes Centre, Colney Lane, Norwich NR4 7UH, UK  
<sup>6</sup>Core Research for Evolutional Science and Technology (CREST), Japan Science and Technology Agency, 4-1-8 Honcho, Kawaguchi, Saitama 332-0112, Japan  
<sup>7</sup>Kazusa DNA Research Institute, 2-6-7 Kazusa-kamatari, Kisarazu, Chiba 292-0818, Japan  
<sup>8</sup>Department of Biological Sciences, Graduate School of Science, The University of Tokyo, 7-3-1 Hongo, Bunkyo, Tokyo 113-0033, Japan

\* These authors contributed equally to this work  
 † Present address: Genetics Institute, Ludwig Maximilians Universität (LMU), Maria-Ward-Str. 1a, D-80638 München, Germany

The roots of most higher plants form arbuscular mycorrhiza, an ancient, phosphate-acquiring symbiosis with fungi, whereas only four related plant orders are able to engage in the evolutionary younger nitrogen-fixing root-nodule symbiosis with bacteria<sup>1</sup>. Plant symbioses with bacteria and fungi require a set of common signal transduction components that redirect root cell development<sup>2,3</sup>. Here we present two highly homologous genes from *Lotus japonicus*, *CASTOR* and *POLLUX*, that are indispensable for microbial admission into plant cells and act upstream of intracellular calcium spiking<sup>4</sup>, one of the earliest plant responses to symbiotic stimulation. Surprisingly, both twin proteins are localized in the plastids of root cells, indicating a previously unrecognized role of this ancient endosymbiont in controlling intracellular symbioses that evolved more recently.

Upon recognition of a bacterial symbiotic signalling molecule, the 'Nod factor', root hairs of leguminous plants reprogramme their development<sup>5,6</sup>. Tip growth is redirected to form a curl that entraps a bacterial microcolony to initiate the formation of the infection thread. These events are preceded by the rapid formation of transient subcellular gradients of proton, potassium, chloride and calcium ions, followed after about 10 min by oscillations in intracellular calcium concentration, the 'calcium spiking' response<sup>7</sup>. We used *Lotus japonicus* mutants to identify the molecular players of this electrochemical prelude to symbiosis. Mutants affected in the *CASTOR* or *POLLUX* genes exhibit very similar phenotypes; they do not form root nodules or arbuscular mycorrhizal symbiosis. Root hairs treated with *Mesorhizobium loti* or Nod factor show branching and tip swelling (Fig. 1a–f, and data not shown), but infection threads are never formed. Similarly, in the arbuscular mycorrhizal symbiosis, fungal entry into root epidermal cells is not supported, and infection attempts are aborted<sup>8–11</sup>. Root hairs of all tested *castor*<sup>12</sup> and *pollux* mutants lacked the Nod-factor-induced calcium spiking that is typically seen with wild-type (Fig. 1g). However, root-hair branching was observed in these non-spiking mutants

(Fig. 1e, f) and so some of the earliest plant responses to Nod factors can be genetically uncoupled. These results demonstrate that *CASTOR* and *POLLUX* act very early in a signal transduction chain leading from the perception of Nod factor to the activation of calcium spiking. They are also required for the execution of the appropriate morphological response of the root hair, because only

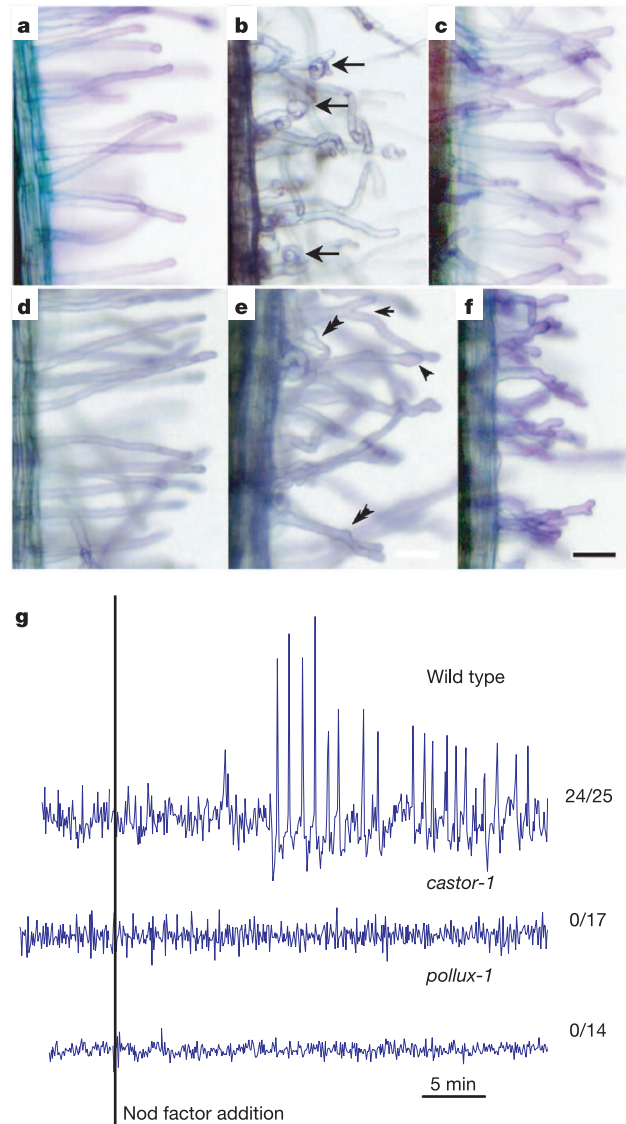


**Figure 1** Phenotypes of *castor* and *pollux* mutants. **a–f**, *L. japonicus* root hair responses induced by *Mesorhizobium loti* TONO inoculation or Nod factor (NF) treatment. Root hairs of wild-type (B-129 Gifu) and *castor* mutants, inoculated with *M. loti* TONO (**b**, **e**) or treatment with 100 nM NF (**c**, **f**) are shown. **a**, **d**, Non-treated control of wild type and *castor-4*, respectively. **b**, Wild-type root hair curling (arrows). **e**, Root hair swelling (arrowhead), tip growth (double arrowheads) and branching (small arrow) on a *castor-5* mutant inoculated with *M. loti*. **c**, **f**, NF-induced root hair deformation, on wild-type and *castor-4* mutant roots, respectively. Scale bar, 50  $\mu$ m. **g**, Analysis of calcium spiking in root hairs. Each trace is from a single root hair using seedlings of the wild type (B-129 Gifu) or of mutants carrying the *castor-1* or *pollux-1* alleles. Root hairs were injected with the calcium-sensitive dye Oregon green-dextran and after about 20 min NF was added at 10 nM. The graph shows typical traces of the differences in fluorescence intensity between 5-s sequential time points. Similar results were seen with the *castor-2*, *castor-3*, *castor-4* and *pollux-2* mutants; the fractions show the number of root hairs inducing calcium spiking relative to the numbers assayed for each locus, with separate plants for each assay.

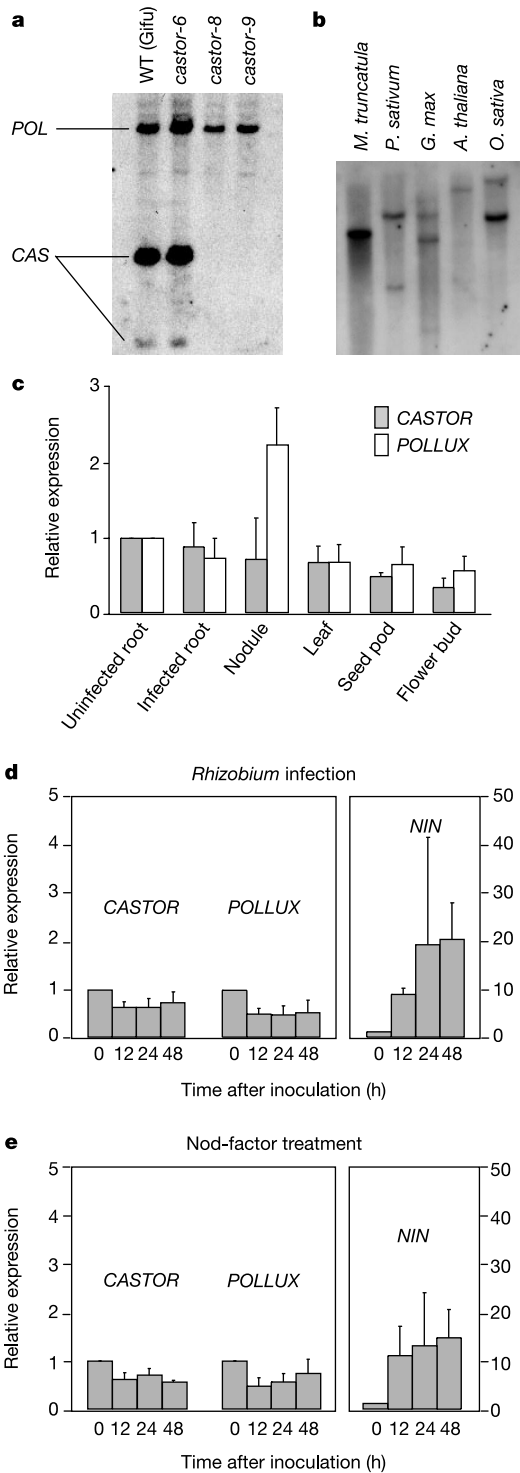


**Figure 2** Southern blot and RT-PCR expression analyses of *CASTOR* and *POLLUX*. **a, b**, DNA gel blot analysis of *CASTOR* (*CAS*) and *POLLUX* (*POL*). **a**, Wild-type (WT; B-129 Gifu) and *castor* mutant alleles (*castor-6*, *castor-8* and *castor-9*). Two distinct signals, representing the *CAS* and *POL* genes, were detected with a *CASTOR* probe on DNA of the wild type or of plants homozygous for point-mutation allele *castor-6*. The fragment representing *CAS* was absent from the DNA of deletion mutants *castor-8* and *castor-9*. **b**, Leguminous and non-leguminous plants. *G. max*, *Glycine max*; *O. sativa*, *Oryza sativa*. Genomic DNAs were digested with *Xba*I (**a**) or *Bam*HI (**b**). **c**, *CASTOR* and *POLLUX* expression in various organs of *L. japonicus* B-129 Gifu. **d, e**, Induction of *CASTOR*, *POLLUX* and *NIN* expression from 0 to 48 h after inoculation with *M. loti* (**d**) or treatment with Nod factor (**e**). Expression strengths are shown relative to uninfected root (**c, d**) or non-treated root (**e**). The error bars indicate standard deviation.

branching and deformation, but not curling or infection thread formation, were observed.

The *CASTOR* and *POLLUX* genes were isolated through positional cloning and by their strong sequence similarity. Using the extensive collection of microsatellite (simple sequence repeat (SSR)) markers available for *L. japonicus*<sup>13</sup>, the *CASTOR* and *POLLUX* genes were positioned close to the bottom ends of chromosomes 1 and 6, respectively. Analysis of the sequence obtained in the context of the genome project<sup>14</sup> revealed very limited local similarity between the *CASTOR* and *POLLUX* genomic regions. Only *CASTOR* and *POLLUX* themselves were conserved, suggesting that the two genes are the product of a limited duplication event (Supplementary Fig. 1).

Five *castor* alleles were independently mapped to the south end of chromosome 1, close to SSR marker TM0105 (ref. 14). Starting with this marker, a bacterial artificial chromosome (BAC)<sup>15</sup>/transformation-competent artificial chromosome (TAC)<sup>14</sup> contig (Supplementary Fig. 1b) was constructed that extended into the telomeric region, as indicated by multiple copies of subtelomeric repeat LjTR4 (M.H., unpublished data) towards the southern extremity (Supplementary Fig. 1b). Genetic mapping was affected by an inversion 145 kilobases (kb) long between the parental lines B-129 and MG-20 (ref. 16) with no recombination events observed on inspection of 1,833 individuals of five different F<sub>2</sub> populations (Supplementary Fig. 1a), delimiting the *CASTOR* locus to a region of about 240 kb. Polymerase chain reaction (PCR) marker TB2R could not be amplified from individuals homozygous for the *castor-8* or *castor-9* alleles. PCR and Southern blot analysis (Fig. 2a) indicated that both alleles have large deletions of more than 20 kb encompassing the *CASTOR* gene, and subsequent sequence analysis revealed that marker TB2R is located in a *CASTOR* intron (Supplementary Fig. 1d).

Sequencing of genomic DNA identified non-silent mutations within the *CASTOR* gene in 15 additional mutants, thus providing a proof of gene identification (Supplementary Table 1). Four independent mutations (*castor-8* to *castor-11*), which arose during tissue culture and are thus attributable to somaclonal variation, were deletions between 1 base pair and more than 20 kb in size (Supplementary Table 1), and not retrotransposon insertions as observed in other *Lotus* somaclonal mutants<sup>17</sup>. This bias might be caused by the proximity to the telomere.

The *POLLUX* gene was found to segregate with SSR marker TM0885 (Supplementary Fig. 1e). A TAC clone carrying SSR TM0885 was completely sequenced, and a candidate gene with high homology to *CASTOR* was identified. Sequencing of nine different symbiosis-defective mutant alleles confirmed the identification of the *POLLUX* gene (Supplementary Table 1).

Full-length complementary DNA (cDNA) sequences corresponding to the *CASTOR* and *POLLUX* genes were obtained through 5' and 3' rapid amplification of cDNA ends and by sequencing of cDNA clones. Alignment of the cDNA with the genomic sequence identified 12 exons for both genes but also the occurrence of alternative splicing (Supplementary Fig. 1d, f). Interestingly, the intron between the seventh and eighth exon was retained in several *CASTOR* cDNA clones, and the presence of this non-spliced intron was also confirmed by reverse transcriptase PCR (RT-PCR) on root and nodule RNA (data not shown). This alternatively spliced mRNA of unknown function encodes a truncated protein of 569 amino acids.

The *POLLUX* gene was detected by genomic DNA-blot analysis using *CASTOR* as a probe (Fig. 2a). *CASTOR*-*POLLUX* homologues exist in one or two copies in other dicotyledonous and monocotyledonous plants (Fig. 2b). Notably, only a single signal was detected in *Medicago truncatula*. This signal probably corresponds to the recently cloned *DMII* gene<sup>18</sup>, whose product is more closely related to *POLLUX* than it is to *CASTOR* (Fig. 3d).

The expression level of *CASTOR* and *POLLUX* mRNA in each

organ and in early stages of symbiosis was examined by quantitative RT-PCR (Fig. 2c–e). *CASTOR* was expressed in all organs, with highest expression in non-infected roots, whereas *POLLUX* expression was enhanced in nodules. *M. loti* inoculation or Nod-factor treatment slightly repressed the expression of *CASTOR* and *POLLUX* genes during the first 2 days. This was in contrast to the *NIN* gene, which is also required for nodulation but whose expression was strongly upregulated (Fig. 2d, e).

*CASTOR* and *POLLUX* encode predicted integral membrane proteins of 853 and 917 amino acids, respectively, with at least four transmembrane (TM) regions (Fig. 3a). Overall the two proteins are very similar to each other with the exception of the amino-terminal regions, which are more divergent (Fig. 3a). However, both proteins carry potential chloroplast transit peptides of 69 and 57 amino acids at their N termini (TargetP scores 0.953 and 0.959), respectively. We confirmed this prediction by using fusions of full-length *CASTOR* or *POLLUX* to green fluorescent protein (GFP). As a positive control, the transit peptide of the *Arabidopsis* plastid protein *recA*<sup>19</sup> (At1g79050) was fused with DsRed2 (*AtrecA*–DsRed2). When this fusion was transiently expressed in onion epidermis or pea root cells together with *CASTOR*–GFP or *POLLUX*–GFP, they localized together, providing strong evidence for the

targeting of *CASTOR* and *POLLUX* to plastids (Fig. 4). Given their high level of sequence similarity and their similar localization it is surprising that they cannot functionally replace each other, because the mutation of either *CASTOR* or *POLLUX* causes a symbiosis-defective phenotype. One possibility is that *CASTOR* and *POLLUX* form heteromeric complexes.

Database searches based on sequence homology did not result in clear functional predictions for the novel proteins, although similar hypothetical proteins from rice and *Arabidopsis* could be detected (Fig. 3). However, searches based on protein structure using FUGUE<sup>20</sup> resulted in significant structural matches to calcium-gated potassium channels such as the *Methanobacterium thermoautotrophicum* MthK, for which a crystal structure has been resolved<sup>21</sup> (Fig. 3b, c). Comparison with MthK revealed that the TM domains flanking the pore are particularly well conserved in the novel plant proteins (Fig. 3b). However, amino-acid replacements in the filter region suggest different ion selectivity. Residues 61–63 in MthK are Gly-Tyr-Gly, a canonical motif in potassium channels, whereas the corresponding residues in *CASTOR* and *POLLUX* are Ser-Gly-Asn (Fig. 3b). Homology modelling of the filter region of *CASTOR* (Fig. 3c) indicates that these differences result in a more helical backbone, and this would modify both the diameter and

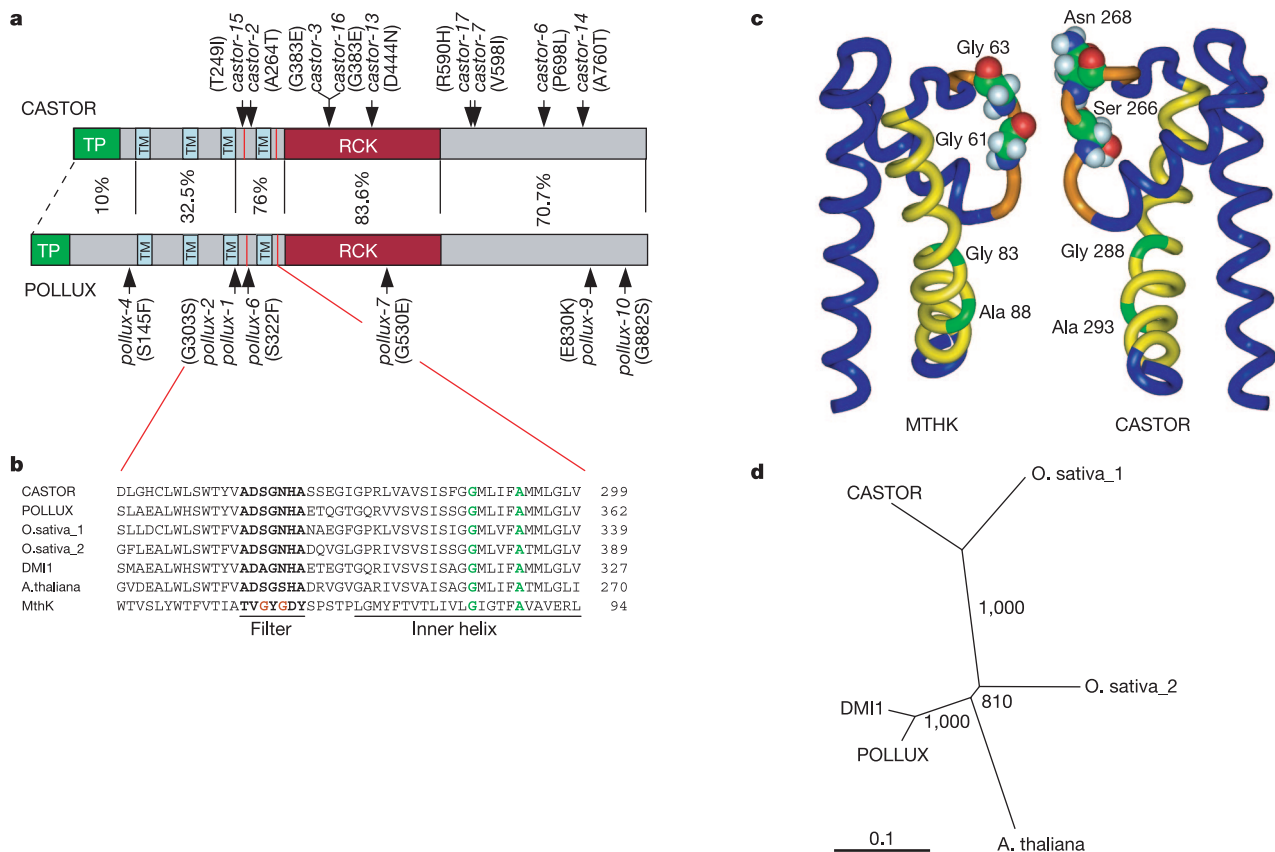


**Figure 3** Structure, domains and homologues of *CASTOR* and *POLLUX*. **a**, Protein domains and local sequence identity between *CASTOR* and *POLLUX*. RCK, region with ~35% similarity to a domain implicated in the regulation of conductance, so far only found in potassium channels; TM, transmembrane helix; TP, chloroplast transit peptide. The position and amino-acid changes of non-symbiotic mutations are shown above and below the bars representing the *CASTOR* and *POLLUX* proteins respectively. **b**, Alignment of the filter and inner helical region of the *Methanobacterium thermoautotrophicum* MthK channel (O27564) with the homologous region of *CASTOR*, *POLLUX* and plant homologues. This region of MthK forms the core of the pore depicted in **c**. **c**, X-ray crystal structure of the ion pore region of the MthK channel, and a model of the homologous region in *CASTOR*. The filter region is coloured orange; inner helices are coloured yellow.

Residues Gly61 and Gly63 in the MthK structure, and the corresponding Ser and Asn residues in *CASTOR*, are shown in space-filling mode to demonstrate the effects of these substitutions on the diameter and electrostatic properties of the pore. Residues Gly83 (the gating hinge<sup>20</sup>) and Ala88 (the narrowest point in the MthK intracellular entryway<sup>20</sup>) in the inner helix are highlighted in green. **d**, Phylogenetic tree of *CASTOR* and *POLLUX* homologues in angiosperms. The N'-truncated amino-acid sequences of *CASTOR*, *POLLUX* and DMI1 (*M. truncatula*), and the most similar proteins in *A. thaliana* (At5g49960) and *Oryza sativa* (*O. sativa\_1*, deduced from AK068216, and *O. sativa\_2*, deduced from AK072312) were aligned with the Clustal W program. Shown is a neighbour-joining tree with 1,000 bootstrap replicates.

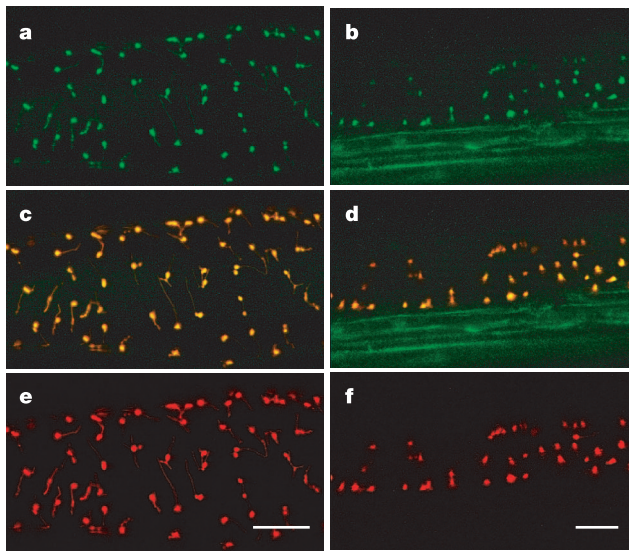


**Figure 4** Intracellular localization of CASTOR and POLLUX. Confocal laser scanning micrographs of onion epidermal cells (**a, c, e**) and pea roots (**b, d, f**), transiently expressing *Atreca*-DsRed2 (**e, f**) with *CASTOR*-GFP (**a**) and *POLLUX*-GFP (**b**) fusions, respectively. In the merged images (**c, d**), the colocalized signals of green GFP fluorescence (**a, b**) and red DsRed2 fluorescence (**e, f**) appear yellow. (**a, c, e**, projection of six optical sections taken at 5- $\mu$ m intervals along the z axis; **b, d, f**, projection of eight optical sections taken at 4- $\mu$ m intervals along the z axis). Green fibrillar cells in **b, d** are seen owing to their autofluorescence. Scale bars, 50  $\mu$ m.

electrostatic properties of the pore (Fig. 3c). Despite these observations, it is difficult to predict the ion selectivity of the pore formed by CASTOR and POLLUX. The proteins also carry a region with homology to the RCK domain, which regulates the conductance of potassium channels in response to changes in cytoplasmic calcium concentration<sup>22</sup>. As with many other ion channels, MthK acts in a multimeric complex<sup>21</sup>. Given these similarities, it is possible that CASTOR and POLLUX also act as multimeric ion channels. The significance of these homologies is supported by the observed accumulation of six amino-acid substitutions in the pore and RCK-like domains that lead to a mutant phenotype (Fig. 3a and Supplementary Table 1). However, the channel activity and ion selectivity of CASTOR and POLLUX have still to be confirmed experimentally.

Our results reveal a new and unexpected aspect of plastid biology. CASTOR and POLLUX are two closely related members of a novel class of plastid-localized proteins that are absolutely required for early signal transduction events leading to endosymbioses. How are these proteins implicated in a process that starts with the perception of microbial signals at the plasma membrane and leads to changes in gene expression in the nucleus, among other responses? The immediate-early symbiont-stimulated ion fluxes occur across the plasma membrane<sup>7</sup>, whereas calcium spiking<sup>4</sup> is typically observed around the nucleus of stimulated root hair cells. Considering their predicted functions and their mutant phenotypes, it seems that CASTOR and POLLUX might mediate ion fluxes between plastids and cytosol that are a prerequisite for calcium spiking. Although in our experiments, pea plastids seemed to be randomly distributed within root cells, others have observed plastid accumulation around the nucleus<sup>23</sup>, so we cannot exclude the plastid as the source of calcium in the spiking response. Determining how the different ion fluxes are orchestrated and how they result in symbiotic changes in root cells will be a challenging research area. Plastids represent the endosymbiotic remnant of a free-living cyanobacterial progenitor. It is fascinating to discover that an 'ancient' endosymbiont helps bacterial and fungal 'newcomers' to infect their partner. □

## Methods

### Plant material

Mutants *Ljsym71-1*, *Ljsym71-2* (ref. 24), *N5*, *N10*, *Ljsym86-1* (M.K., unpublished data), *Ljsym4-2* (ref. 10), *Ljsym22-1*, *Ljsym23-1*, *Ljsym23-2* (ref. 9) and lines with the prefix 'SL' identified through TILLING<sup>25</sup>, were isolated from four independent EMS-mutagenesis experiments of *L. japonicus* B-129 Gifu. Non-nodulating mutants *G00472*, *G00716*, *G00862* (derived from B-129) and *M89-27* (from MG-20) were identified from a screen of plants regenerated from cell cultures of *L. japonicus* (Y.U., unpublished data). Mutant *Ljsym4-1* was generated by T-DNA transformation of *L. japonicus* B-129 Gifu, but the gene was not tagged<sup>26</sup>.

### Root hair deformation assay

Root hair deformation was examined as described previously<sup>27</sup>. In brief, 3-day-old seedlings were inoculated with *M. loti* TONO and grown on a filter paper placed on agar medium (nitrogen-free; B&D<sup>28</sup>) for 3 days. For Nod factor application, 2-day-old seedlings were grown for 1 day on an agar-covered glass slide with the lower edge immersed in B&D liquid medium, followed by the application of 100 nM Nod factor and incubation for another 24 h. The roots were stained briefly in 0.001% toluidine blue and examined under a binocular microscope. Observation was repeated at least three times, using five to ten seedlings each.

### Calcium spiking

Seedlings of *L. japonicus* were germinated, mounted and microinjected with Oregon green-dextran dye essentially as described<sup>12</sup>. Fluorescence was imaged with a Nikon TE2000U inverted microscope coupled to a Hamamatsu Photonics digital charge-coupled device camera. The excitation wavelength of 488 nm with an 11-nm bandpass was selected with an Optoscan Monochromator (Cairn Research, Faversham, Kent, UK) and an emission filter of 545  $\pm$  15 nm was used. Images were collected every 5 s with a 200-ms exposure with the use of MetaFluor software, and derivative traces were generated with Microsoft Excel. After microinjection, root hairs were left for at least 20 min before the addition of Nod factor, and only cells showing active cytoplasmic streaming were used for analysis. Nod factors, isolated from a reverse-phase C<sub>18</sub> column, were added directly to the incubation chamber to give an estimated final concentration of 10 nM (ref. 29). Representative traces were selected from at least ten independent cells.

### Positional cloning

*CASTOR* was mapped with six independent F<sub>2</sub> mapping populations, resulting from crosses between *L. japonicus* B-129 Gifu mutants *Ljsym71-2*, *N5*, *Ljsym4-2* or *G00472*, *G00716* and MG-20 Miyakojima, and a cross of *Ljsym4-2* and *L. filicaulis*. The sizes of each F<sub>2</sub> population were 1,563 (*Ljsym71-2*), 190 (*N5*), 180 (*Ljsym4-2*  $\times$  MG-20), 40 (*G00472*), 40 (*G00716*) and 1,514 (*Ljsym4-2*  $\times$  *L. filicaulis*). In total, 3,527 F<sub>2</sub> individuals were analysed with markers flanking *CASTOR*. *POLLUX* was mapped with three independent F<sub>2</sub> mapping populations. The sizes of each population of F<sub>2</sub> were 531 (*Ljsym23-2*  $\times$  MG-20), 292 (*Ljsym86-1*  $\times$  MG-20) and 409 (*Ljsym23-1*  $\times$  *L. filicaulis*).

### Southern blot and expression analysis

A 573-base-pair fragment of *CASTOR* was amplified with the primer 5' -TCAAAGAAGGA TTACGAGGA-3' in combination with 5' -AATTTTACCACCATAAGATGC-3'. Genomic DNA (10  $\mu$ g) was extracted from leaves and digested with *Xba*I or *Bam*HI. Probe labelling and signal detection were performed with AlkPhos Direct (Amersham).

The expression of the *CASTOR* gene was analysed by quantitative RT-PCR with the primers *polyubiquitin* (5' -ATGCAGATCTTCGTCAGACAGCTTGAC-3' / 5' -ACCTCCCC TCAGACGAAGGA-3'), *NIN* (ref. 6) (5' -TGGATCAGCTAGCATGGAAT-3' / 5' -TCTGCTTCTGCTGTGTGTCAC-3'), *CASTOR* (5' -ATGTGGCCTTGACATAAG-3' / 5' -AGTGACGACGTATAACAGCA-3') and *POLLUX* (5' -AGGTATCCTAGGGAAAAAGC-3' / 5' -TTACTCTCCTGGTTCTCTCC-3'). Total RNA was extracted with the RNeasy Mini kit (Qiagen) and treated with DNase I (Takara). Real-time RT-PCR was performed in GeneAmp 5700 (Applied Biosystems) with a Quantitect SYBR Green RT-PCR kit (Qiagen). Expression levels were normalized on the basis of the amount of *polyubiquitin* transcripts. All values are means and standard deviations for three replicates of three biological repeats.

### Construction of fluorescence-tagged fusions

cDNA fragments of *CASTOR* and *POLLUX* were amplified by PCR with the primers CAS-F/CAS-R (5' -ACGCGTCGACATGTCTTGGATTCCGGAG-3', 5' -CATGCCATGGATT CCTTTTCAGTAATTAC-3') and POL-F/POL-R (5' -ACGCGTCGACATGATACCCT ACCAGTA-3', 5' -CATGCCATGGAATCGCCTGAAGCAATCAC-3'), respectively. Each fragment was digested with *Sal*I and *Nco*I and ligated into the same restriction sites of pUC18-CaMV35S-sGFP (S65T)-nos<sup>30</sup>. For the construction of *Atreca*-DsRed2 fusion, a fragment encoding the transit peptide of *Atreca*<sup>19</sup> was amplified from *Arabidopsis thaliana* genomic DNA with the use of the primers *Atreca*-*Sal*I-F/*Atreca*-LFH-R (5' -ACGCGT CGACATGGATTACAGCTAGTC-3', 5' -ATCGAATTCAGAACTGATTTTGTG-3'). DsRed2 fragment was amplified from pDsRed2-1 (Clontech) with the use of DsRed2-LFH-F/DsRed2-*Not*I-R (5' -CTGAATTCGATCGCGACATGGCCTCCTCCGAGAA-3', 5' -ATTGCGCGCCCTACAGGAACAGGTGGTG-3') primers. *Atreca*-LFH-R and DsRed2-LFH-F primers were designed to introduce overlapping nucleotides (underlined) at the 3' and 5' ends of the *Atreca* and DsRed2 fragments, respectively. Using both fragments as templates, joint PCR was performed with *Atreca*-*Sal*I-F and DsRed2-*Not*I-R primers. The resulting fusion fragment was digested with *Sal*I and *Not*I and cloned into the same restriction site of pUC18-CaMV35S-sGFP (S65T)-nos vector.

**Microprojectile bombardment and confocal laser scanning microscopy**

Microprojectile bombardment was performed with a Biolistic PDS-1000/He Particle Delivery System (Bio-Rad). Epidermis of *Allium cepa* scaly bulb and roots of *Pisum sativum* were bombarded with a rupture-disk pressure of 1,100 p.s.i. (~7.6 MPa) at a target distance of 6 cm. At 24–40 h after bombardment, they were analysed with a Bio-Rad Radiance2000 confocal laser scanning microscope. Green fluorescence of GFP and red fluorescence of DsRed2 were excited at 488 nm with an argon laser and collected sequentially with a filter set (HQ530/60 and E570LP). Images of both fluorescences were processed and merged with the Lasersharp2000 program system (Bio-Rad).

**Computer analysis**

Sequences were analysed by BLAST (<http://www.ncbi.nlm.nih.gov/BLAST/>) and GENSCAN version 1.0 (<http://genes.mit.edu/GENSCAN.html>). Clustal W (<http://www.ebi.ac.uk/clustalw/>) was used for multiple alignment and evolutionary relationships. The target peptide and transmembrane regions were predicted by TargetP version 1.01 (<http://www.cbs.dtu.dk/services/TargetP/>) and TMHMM version 2.0 (<http://www.cbs.dtu.dk/services/TMHMM-2.0/>). For domain and structure analyses, both Pfam (<http://www.sanger.ac.uk/Software/Pfam/>) and FUGUE v.2.0 (<http://www-cryst.bioc.cam.ac.uk/~fugue/>) were applied.

Received 30 September; accepted 29 November 2004; doi:10.1038/nature03237.  
Published online 22 December 2004.

1. Smith, S. E. & Read, D. J. *Mycorrhizal Symbiosis* (Academic, London, 1997).
2. Oldroyd, G. E. D. Dissecting symbiosis: developments in Nod factor signal transduction. *Ann. Bot.* **87**, 709–718 (2001).
3. Kistner, C. & Parniske, M. Evolution of signal transduction in intracellular symbiosis. *Trends Plant Sci.* **7**, 511–518 (2002).
4. Ehrhardt, D., Wais, R. & Long, S. Calcium spiking in plant root hairs responding to Rhizobium nodulation signals. *Cell* **85**, 673–681 (1996).
5. Truchet, G. *et al.* Sulphated lipooligosaccharide signals from *Rhizobium meliloti* elicit root nodule organogenesis in alfalfa. *Nature* **351**, 670–673 (1991).
6. Radutoiu, S. *et al.* Plant recognition of symbiotic bacteria requires two LysM receptor-like kinases. *Nature* **425**, 585–592 (2003).
7. Cárdenas, L. *et al.* Ion changes in legume root hairs responding to Nod factors. *Plant Physiol.* **123**, 443–452 (2000).
8. Senoo, K. *et al.* Isolation of two different phenotypes of mycorrhizal mutants in the model legume plant *Lotus japonicus* after EMS-treatment. *Plant Cell Physiol.* **41**, 726–732 (2000).
9. Szczyglowski, K. *et al.* Nodule organogenesis and symbiotic mutants of the model legume *Lotus japonicus*. *Mol. Plant Microbe Interact.* **11**, 684–697 (1998).
10. Bonfante, P. *et al.* The *Lotus japonicus* *LjSym4* gene is required for the successful symbiotic infection of root epidermal cells. *Mol. Plant Microbe Interact.* **13**, 1109–1120 (2000).
11. Novero, M. *et al.* Dual requirement of the *LjSym4* gene for mycorrhizal development in epidermal and cortical cells of *Lotus japonicus* roots. *New Phytol.* **154**, 741–749 (2002).
12. Harris, J. M., Wais, R. & Long, S. R. *Rhizobium*-induced calcium spiking in *Lotus japonicus*. *Mol. Plant Microbe Interact.* **16**, 335–341 (2003).
13. Hayashi, M. *et al.* Construction of a genetic linkage map of the model legume *Lotus japonicus* using an intraspecific F2 population. *DNA Res.* **8**, 301–310 (2001).
14. Nakamura, Y. *et al.* Structural analysis of a *Lotus japonicus* genome. II. Sequence features and mapping of sixty-five TAC clones which cover the 6.5-mb regions of the genome. *DNA Res.* **9**, 63–70 (2002).
15. Kawasaki, S. & Murakami, Y. Genome analysis of *Lotus japonicus*. *J. Plant Res.* **113**, 497–506 (2000).
16. Kawaguchi, M. *et al.* Providing the basis for genomics in *Lotus japonicus*: the accessions Miyakojima and Gifu are appropriate crossing partners for genetic analyses. *Mol. Gen. Genomics* **266**, 157–166 (2001).
17. Stracke, S. *et al.* A plant receptor-like kinase required for both fungal and bacterial symbiosis. *Nature* **417**, 959–962 (2002).

18. Ane, J. M. *et al.* *Medicago truncatula* *DMI* required for bacterial and fungal symbioses in legumes. *Science* **303**, 1364–1367 (2004).
19. Köhler, R. H. *et al.* Exchange of protein molecules through connections between higher plant plastids. *Science* **276**, 2039–2042 (1997).
20. Shi, J., Blundell, T. L. & Mizuguchi, K. FUGUE: sequence-structure homology recognition using environment-specific substitution tables and structure-dependent gap penalties. *J. Mol. Biol.* **310**, 243–257 (2001).
21. Jiang, Y. *et al.* Crystal structure and mechanism of a calcium-gated potassium channel. *Nature* **417**, 515–522 (2002).
22. Jiang, Y. *et al.* Structure of the RCK domain from the *E. coli* K<sup>+</sup> channel and demonstration of its presence in the human BK channel. *Neuron* **29**, 593–601 (2001).
23. Kwok, E. Y. & Hanson, M. R. Plastids and stromules interact with the nucleus and cell membrane in vascular plants. *Plant Cell Rep.* **23**, 188–195 (2004).
24. Kawaguchi, M. *et al.* Root, root hair, and symbiotic mutants of the model legume *Lotus japonicus*. *Mol. Plant Microbe Interact.* **15**, 17–26 (2002).
25. Perry, J. A. *et al.* A TILLING reverse genetics tool and a web-accessible collection of mutants of the legume *Lotus japonicus*. *Plant Physiol.* **131**, 866–871 (2003).
26. Schaefer, L. *et al.* Symbiotic mutants deficient in nodule establishment identified after T-DNA transformation of *Lotus japonicus*. *Mol. Gen. Genet.* **259**, 414–423 (1998).
27. Niwa, S. *et al.* Responses of a model legume *Lotus japonicus* to lipochitin oligosaccharide nodulation factors purified from *Mesorhizobium loti* JRL501. *Mol. Plant Microbe Interact.* **14**, 848–856 (2001).
28. Broughton, W. J. & Dilworth, M. Y. Control of leghemoglobin synthesis in snake beans. *Biochem. J.* **125**, 1075–1080 (1971).
29. Firmin, J. L. *et al.* Resistance to nodulation of cv. Afghanistan peas is overcome by nodX, which mediates an O-acetylation of the *Rhizobium leguminosarum* lipo-oligosaccharide nodulation factor. *Mol. Microbiol.* **10**, 351–360 (1993).
30. Isono, K. *et al.* Leaf-specifically expressed genes for polypeptides destined for chloroplasts with domains of  $\sigma^{70}$  factors of bacterial RNA polymerases in *Arabidopsis thaliana*. *Proc. Natl Acad. Sci. USA* **94**, 14948–14953 (1997).

**Supplementary Information** accompanies the paper on [www.nature.com/nature](http://www.nature.com/nature).

**Acknowledgements** We thank K. Szczyglowski, J. Webb and J. Stougaard for providing mutant seeds; M. Hayashi for help with mapping; T. Kojima and R. Ohtomo for mycorrhiza analysis; Y. Niwa for providing pUC18-CaMV35S-sGFP (S65T)-nos vector; G. Oldroyd and J. Sun for help with Ca-spiking assays; J. Krüger and B. B. H. Wulff for critical reading of the manuscript; J. Soll for providing the pea root transformation protocol before publication; and M. Durrant for help with modelling the CASTOR pore structure. Part of this work was supported by the fund of Promotion of Basic Research Activities for Innovative Biosciences (BRAIN), and Core Research for Evolutional Science and Technology (CREST), Japan Science and Technology Agency. Research at the Sainsbury Laboratory is funded by the Gatsby Charitable Foundation.

**Competing interests statement** The authors declare that they have no competing financial interests.

**Correspondence** and requests for materials should be addressed to S.K. ([kawasa@nias.affrc.go.jp](mailto:kawasa@nias.affrc.go.jp)). The sequences have been deposited at the DNA Data Bank of Japan with the following accession numbers: LjT02K14a (AP006732), LjT02K14b (AP006733), LjT02K14c (AP006734), LjT45I15 (AP006736), LjT20F11 (AP006737), LjT46G19 (AP006735), LjT45B09a (AP006729), LjT45B09b (AP006730) and LjT45B09c (AP006731); genomic sequences (B-129 Gifu) of CASTOR (AB162016), POLLUX (AB162017), and mRNA sequences (B-129 Gifu) of CASTOR (AB162157) and POLLUX (AB162158).